NASA Technical Paper 1852

Proton-Induced Noise in Digicons

L. Cole Smith, Jacob Becher,
Walter B. Fowler, and Keith Flemming

AUGUST 1981

NASA

NASA Technical Paper 1852

Proton-Induced Noise in Digicons

L. Cole Smith and Jacob Becher
Old Dominion University
Norfolk, Virginia

Walter B. Fowler and Keith Flemming
Goddard Space Flight Center
Greenbelt, Maryland

NASA
National Aeronautics
and Space Administration

Scientific and Technical
Information Branch

1981

All measurement values are expressed in the International System of Units (SI) in accordance with NASA Policy Directive 2220.4, paragraph 4.

ABSTRACT

The Space Telescope (ST), which carries four Digicons, will pass several times per day through a low-altitude portion of the radiation belt called the South Atlantic Anomaly (SAA). This is expected to create interference in what is otherwise anticipated to be a noise-free device. Two essential components of the Digicon, the semiconductor diode array and the UV transmitting window, generate noise when subjected to medium-energy proton radiation, a primary component of the belt. These trapped protons, having energies ranging from 2 to 400 Mev and fluences at the Digicon up to 4,000 P+/sec-cm^2, pass through both the window and the diode array, depositing energy in each.

In order to evaluate the effect of these protons, engineering test models of Digicon tubes to be flown on the High Resolution Spectrograph (HRS) were irradiated with low-flux (10^4 - 10^5 P+/sec-cm^2) monoenergetic proton beams at the University of Maryland cyclotron. Electron-hole pairs produced by the protons passing through the diodes or the surrounding bulk caused a background count rate. This is the result of holes diffusing over a distance of many diode spacings, causing counts to be triggered simultaneously in the output circuits of several adjacent diodes. Pulse-height spectra of these proton-induced counts indicate that most of the bulk-related counts overlap the single photoelectron peak. A geometrical model will be presented of the charge collection characteristics of the diode array that accounts for most of the observed effects.

CONTENTS

ILLUSTRATIONS

ILLUSTRATIONS (Continued)

TABLE

PROTON-INDUCED NOISE IN DIGICONS

L. Cole Smith, Jacob Becher
Old Dominion University
Norfolk, Virginia
and
Walter B. Fowler, Keith Flemming
Laboratory for Astronomy and Solar Physics
Goddard Space Flight Center
Greenbelt, Maryland

INTRODUCTION

The Space Telescope (ST), scheduled for launch aboard the shuttle sometime in 1985, will carry into earth orbit optical-electronic detectors of unprecedented sensitivity. Among these will be digital imaging detectors, or Digicons, which will form an integral part of the High Resolution Spectrograph (HRS), and the Faint Object Spectrograph (FOS). They will perform the essential function of acquiring the observational images photon-by-photon and converting these images into telemetry streams for transmission to earth. The trajectory for the ST calls for the unavoidable passage, about ten times per day, through the lowest part of the inner radiation belt called the South Atlantic Anomaly (SAA). This will expose the scientific instruments to belt electrons, which can be shielded against, and penetrating protons having an energy spectrum at the Digicon ranging from 2 to 400 Mev.

Our studies are continuing on limitations to Digicon operation while in the SAA. Studies so far have indicated that optical materials and semiconductor arrays, used in the construction of the Digicons, display radiation-induced noise when individually irradiated with protons in a test environment.[1] Specifically, our studies have isolated two components which primarily contribute to this noise:

- UV window materials used in the HRS faceplate (MgF2 and LiF) have well-known luminescence bands in the spectral region from 110 to 300 nanometers, which are excitable by a broad range of proton energies. Since these spectral bands coincide with the wavelength region where many faint astrophysical targets-of-opportunity exist, the magnitude can limit the sensitivity of the tube, and hence the faintest objects observable while in the SAA.

- Low-flux proton irradiation of a breadboard diode array target, similar to the 512 element array to be used in the HRS Digicon, has suggested that previously suspected multidiode crosstalk effects exist. By crosstalk is meant the simultaneous activation of several adjacent diodes by one triggering event. This was associated with the ionization from protons passing through the substrate with resulting charges rapidly diffusing towards many different diodes. The resulting counts enhance the radiation sensitivity of the diode array.

We have conducted further radiation tests using a full-scale Digicon tube operating as closely as possible to the final flight configuration. For this purpose, two engineering model Digicons made by Electron Vision Company (EVC) were used in joint tests conducted by Old Dominion University and Goddard Space Flight Center at the University of Maryland cyclotron. The first series of tests conducted in December 1979 utilized a Digicon containing a cesium iodide photocathode on a 4-mm-thick lithium fluoride window. This tube was designated E3 by Goddard. Tests conducted in June 1980 used a MgF2/CsTe Digicon designated E4. Both types of Digicon will be flown together on the HRS and will serve to cover the UV spectrum from 110 nm to 320 nm. In our tests, Digicon E3 was used for initial radiation sensitivity measurements of window/diode array. After these tests suggested potential problems involving diode crosstalk, follow-up studies using Digicon E4 were conducted.

In orbit, the HRS Digicon diode array will be exposed to protons having an average energy spectrum as shown in Figure 1. This spectrum was calculated for a 600-km circular orbit during solar mini-

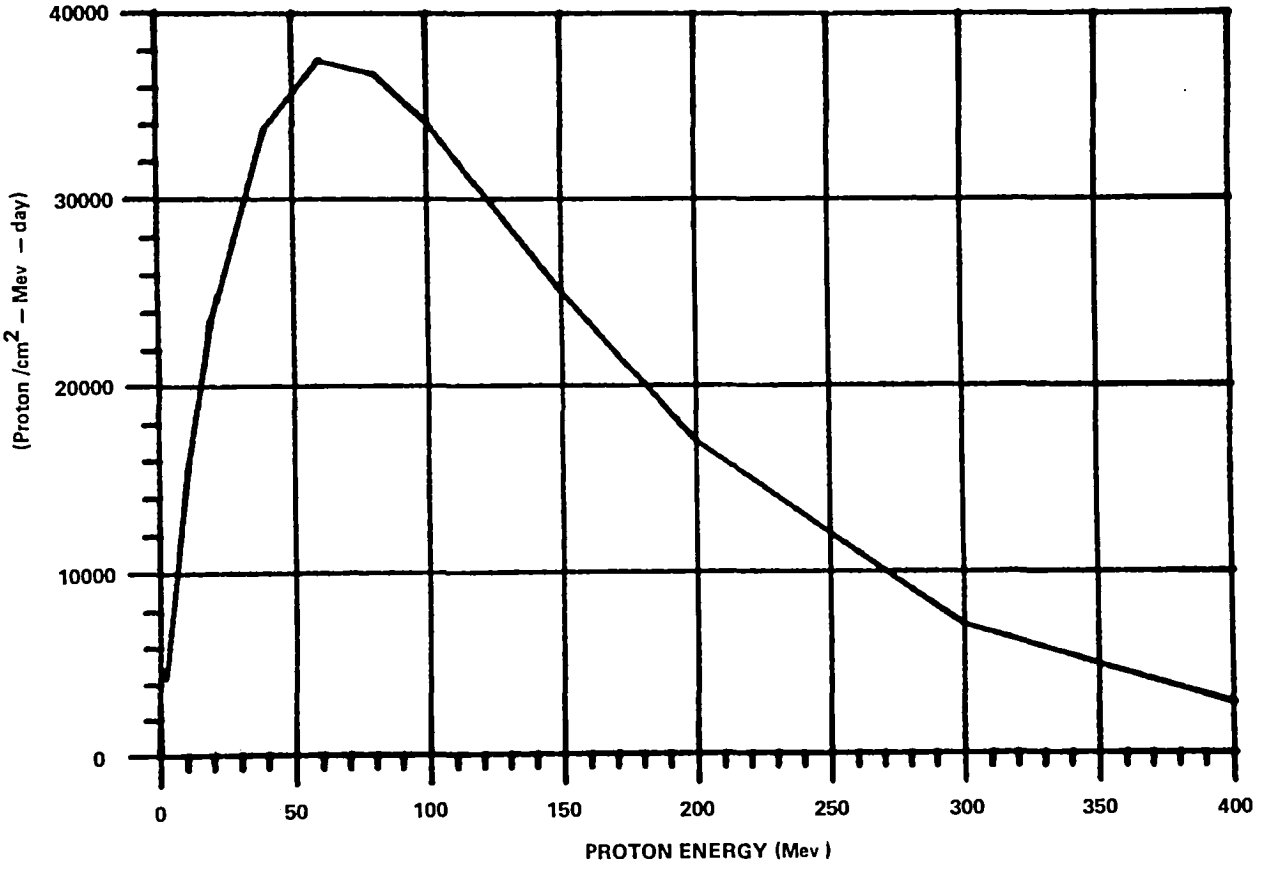

Figure 1. Energy spectrum of protons, integrated over 24 hours, incident at High Resolution Spectrograph (HRS) Digicon diode array.

mum using standard codes developed at Science Applications, Inc. (SAI).* Shielding afforded by the spacecraft and the Digicon itself has been introduced through an approximation utilizing six solid angle-shielding sectors having thicknesses ranging from 2-13 gm/cm**2. Outside the Digicon, at the faceplate, the spectral distribution of energies is about the same with the flux slightly higher. This reference spectrum should be multiplied by a factor of 24 to yield the peak belt spectrum near the center of the SAA, where maximum interference is expected. The reference spectrum peaks between 40 and 80 Mev at around 40,000 p+/cm**2-Mev-day, but includes energies ranging from 2 Mev to a very penetrating 400 Mev.

Our tests utilized monoenergetic proton beams (40 and 85 Mev) with fluences comparable to those anticipated while in the SAA, (roughly 10**3 - 10**4 p+/cm**2-sec, obtained by integrating over the entire peak belt energy spectrum). These tests provided a more realistic data base from which to develop orbital projections and will provide us with information necessary to develop a physical model of the interaction between the protons and diode array. The aim of this model, which is currently under development, is to predict the effects of radiation environments impossible or impractical to simulate on earth.

TEST CONFIGURATION

Although the Digicon has been described in review articles elsewhere,[2,3] a brief description here is in order. In normal operation, a spectral image is focused onto the transmission photocathode at the front end of the detector (Figure 2). Essentially a digital imaging device, the HRS Digicon is a multichannel parallel-output photon detector that uses a thin silicon diode array target to detect accelerated photoelectrons from a UV-sensitive photocathode. Ejected photoelectrons are accelerated through about a 20-kilovolt potential and are magnetically focused by a rare-earth permanent magnet assembly onto a linear target array of 512 solid-state diffused diodes. Each of these diodes consists of a thin p+ n junction embedded in a 400-micron-thick, n-type (rho = 4.5 ohm-cm) silicon substrate to which a 5-volt reverse biasing potential is applied. On tubes E3 and E4, each diode measured 40 microns wide x 250 microns long and was spaced at 50-micron intervals. The geometrical arrangement of the diodes on the array is shown in Figure 3.

When biased, each diode forms a depletion layer having a depth of between two and three microns. A cutaway view of the array is shown in Figure 4. Every electron that is stopped in the depletion zone results in the release of a charge pulse of several thousand electron-hole pairs. The presence of large electric fields in this region results in rapid collection of this charge onto the aluminum electrodes deposited over about a third of the surface of each diode. Further amplification and signal-processing electronics digitize the electron-hole cascade from each diode independently into a form suitable for memory storage.

Using deflection coils driven by a 12-bit D/A converter, the location on the photocathode from which an electron image originates can be stepped along X and Y. This raster-scanning capability will be used during the acquisition of the spectrum of a faint astronomical source to enhance resolution, suppress diode nonuniformity and introduce redundancy in the event of a bad diode. In our tests, this capability was extremely useful in allowing us to map the distribution of luminescence in the faceplate of the tube.

*Private Communication from Charles Hill, S.A.I., Huntsville, Alabama, 1980.

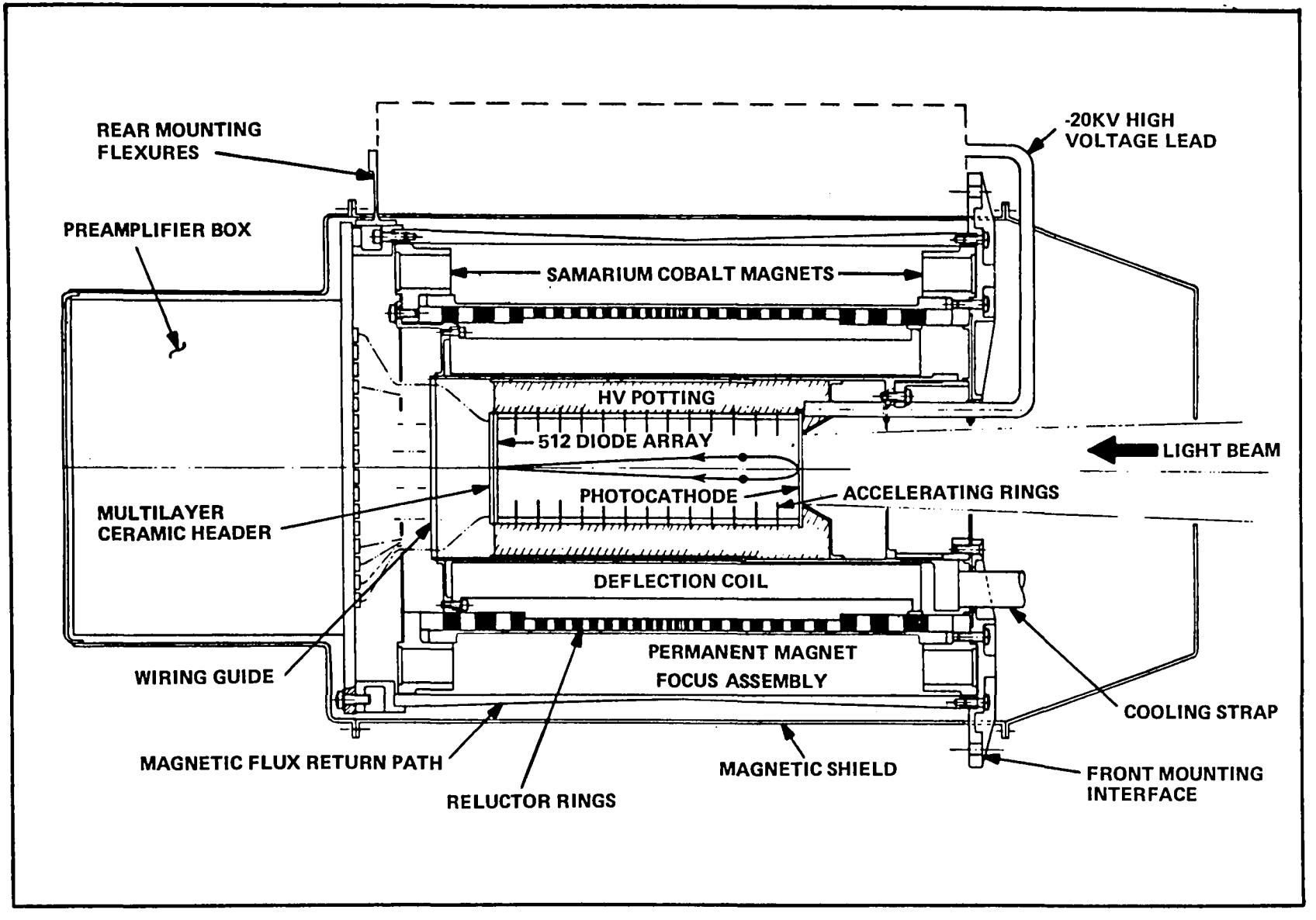

Figure 2. Cross-sectional view of HRS Digicon detector assembly.

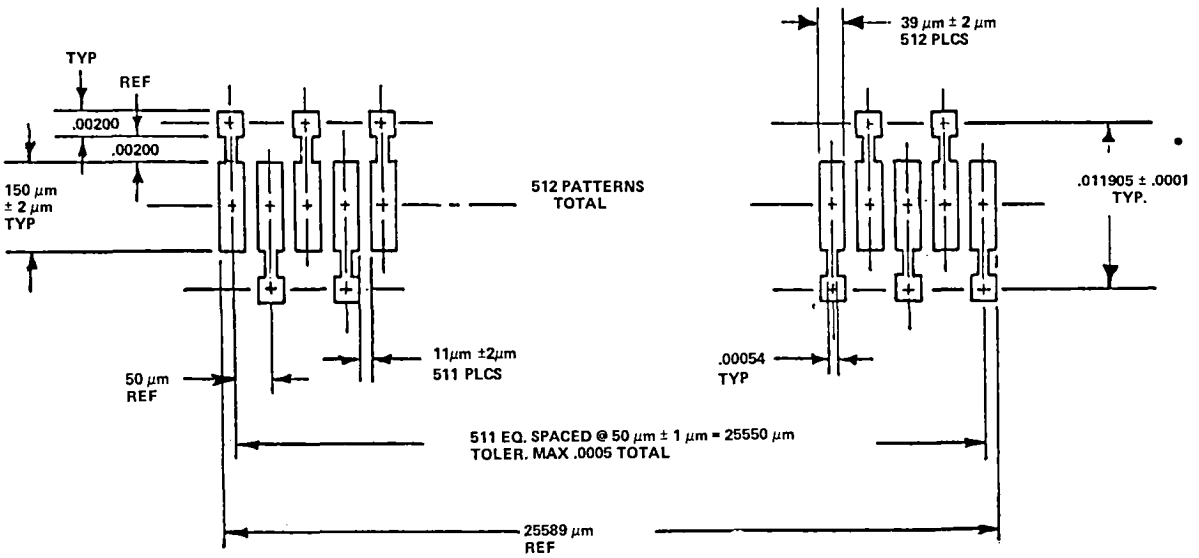

Figure 3. Geometrical arrangement of diodes on the array.

The test configuration is shown in Figure 5. Collimated proton beams of < 1 cm**2 cross section were directed onto the center of the faceplate at the front of the Digicon, which was located inside a scattering chamber and securely bolted onto a movable arm. The Digicon was free to rotate around an axis centered on the photocathode, allowing the rear of the tube to be swung out of the path of the proton beam. This allowed monitoring of the luminescence in the window without the strong interference created by protons penetrating the window and striking the diode array. To monitor the direct proton bombardment of the array, the arm could be returned to zero degrees very quickly, and the high voltage (hv) removed. With the photoelectron background thus eliminated, data accumulation could be resumed. By choosing angles between 0.0 and 10.0 degrees, various portions of the diode array could be brought into the path of the beam. This arm could be remotely controlled in increments of 0.1 degrees and to about the same accuracy. Proton rates were measured using a silicon surface barrier detector (SBD) mounted a few centimeters in front of the faceplate. Sheets of polaroid film were exposed to obtain beam area and proton flux in particles/cm**2-sec.

Although intended to operate with 512 fully independent diode channels, the Digicon could be tested effectively with a small fraction of these diodes active. Ten of the 512 diodes available were monitored through the use of a charge-sensitive hybrid preamp connected to each diode through a multipin header at the base of the tube. Since the December run at Maryland was concerned with monitoring the UV luminescence in the faceplate, it was necessary to choose 10 diodes spread over the entire array so that only Y-axis deflections would be needed to map out the cathode area. On tube E3, in order of position, these 10 diodes were: 11, 67, 128, 240, 243, 320, 379, 451, 452.

After results from these tests indicated the advisability of studying the effects of individual protons on closely spaced diodes, a different diode configuration was chosen for E4 in June. For these

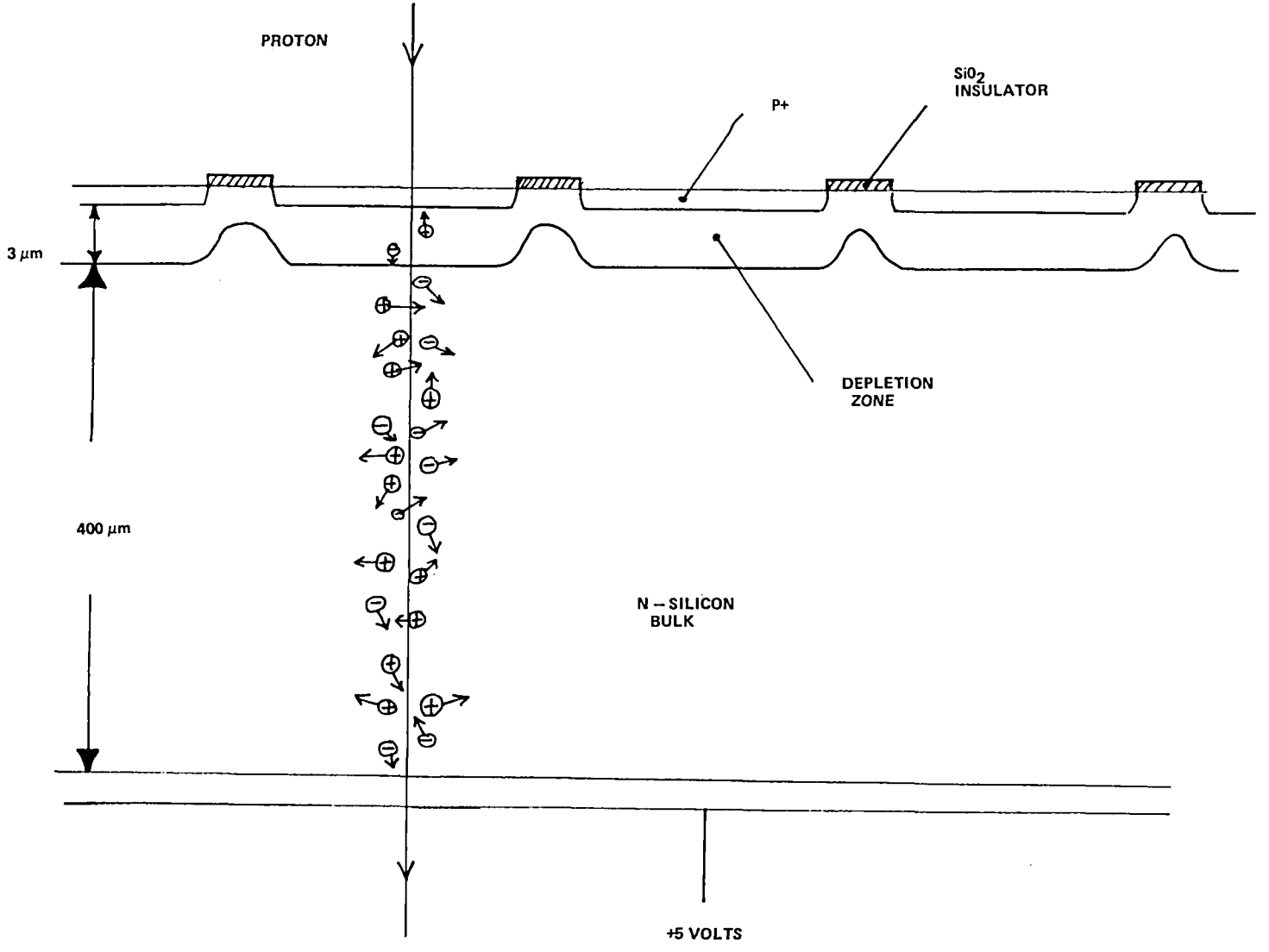

Figure 4. Cutaway view of diodes. P+ layer is about 0.7 μ. Vertical scale is exaggerated.

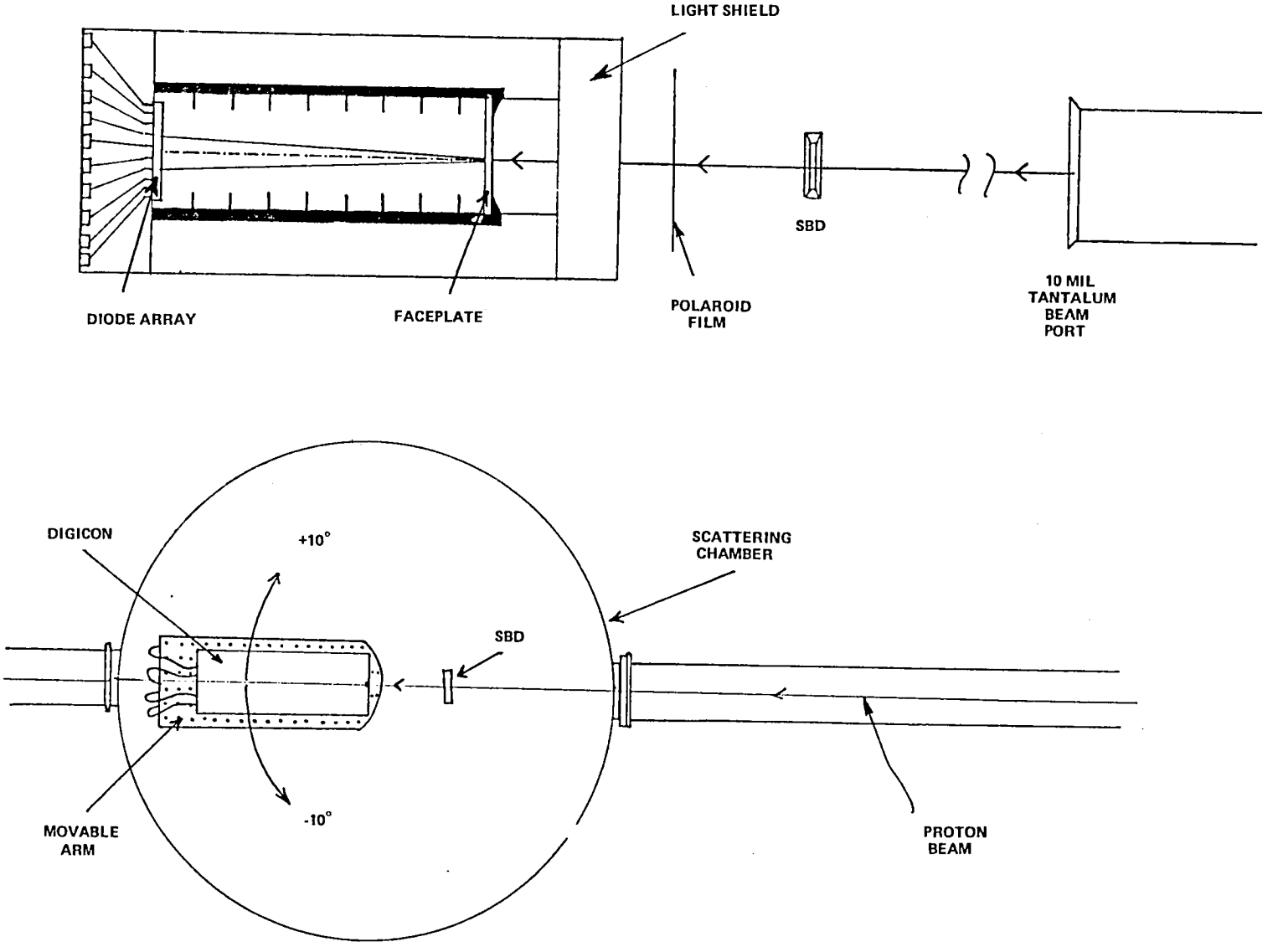

Figure 5. Test configuration used during proton irradiation of HRS Digicon. The tube could be rotated in 0.1° increments up to ± 10°, thus allowing the diode array to be swung into or out of the proton beam.

tests, it was desirable to monitor many adjacent diode pairs to check for crosstalk and other geometrically related effects, resulting in the diode configuration indicated for Digicon E4 in Figure 6. These diodes were chosen to lie near the optical axis of the tube, which during the tests coincided with the proton beam axis.

Each preamp was followed by a chain of electronics containing a pulse shaper, amplifier, discriminator, rate limiter, and 16-bit count accumulator. Under computer software control, pulses from each diode were individually accumulated for a preselected time interval (10 milliseconds or longer), at the end of which time the accumulators were disabled and latched into a set of 10 parallel-to-serial shift registers. The microprocessor controlling these events then listed the counts from the diodes on a line printer and at the end of each run, stored all the data on floppy disks for later retrieval and analysis. Pulse-height analysis from any diode channel was possible, using switchable analog channels placed just after the charge-sensitive preamps. As many as three diodes were monitored simultaneously, allowing measurement of coincidence rates between any pair or all three.

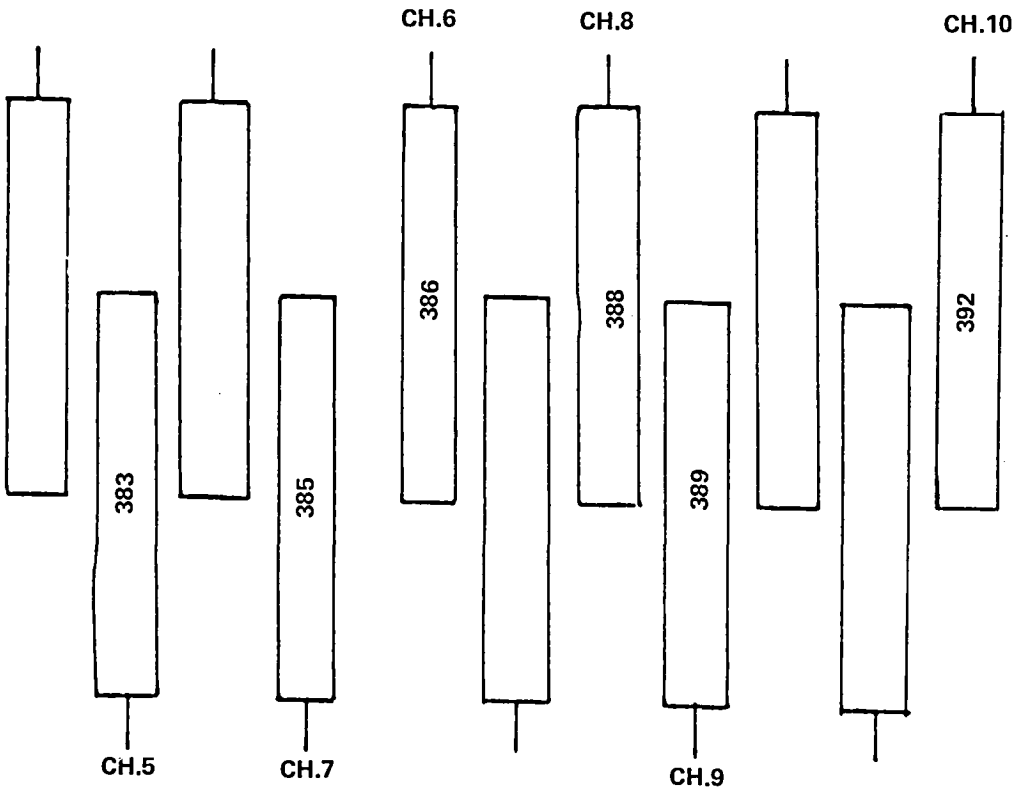

Figure 6. Digicon E4: Six diodes out of the ten available were connected as shown.

Both Digicons were operated with diode bias and/or accelerating voltage, either off or on. This allowed a number of degrees of freedom in measuring the effects of differing depletion layer thicknesses, and in observing both photoelectrons and protons interacting with the diode array together or separately. Diode bias was typically +5 volts and tube voltage from 20-22 kilovolts. A UV penlight and shadow mask were available for internal calibration and diode uniformity checks.

Test procedures consisted of exposing the Digicon tube to monoenergetic collimated proton beams of varying fluences (10**4 - 10**5 p+/cm**2-sec) and energies (40 and 85 Mev), and at various angles of incidence to the faceplate, as indicated in Figure 5. Although these fluences were slightly higher than those expected in the SAA (this was necessary due to time constraints on the use of the cyclotron), no significant deviation from the results presented here is expected at lower fluences.

Tests were divided into the following categories:

- Faceplate fluorescence mapping
- Proton bombardment of the diode array

This choice essentially reflects the expected problem areas and determines the nature of the experimental configuration necessary to acquire the data.

It should be noted that although the primary beam energies used in the tests were 85 and 40 Mev, passage of the beam through a 10-mil tantalum window used to isolate the beam line, as well as 0.5 meters of air, the SBD and a few low-density light shields, reduced the primary proton energies entering the window to 82 and 32 Mev, respectively. Passage through the MgF2/LiF window further reduced these energies to 77 and 20 Mev.

RESULTS

Window Fluorescence

UV window fluorescence and diode background tests were conducted on Digicons E3 and E4 by irradiating the tubes. Angles of 0, 2, 5, and 10 degrees were used to separate these two effects and to reveal their relative magnitude. For configurations in which the diode array was not directly in the proton beam (angles $>$ 5 degrees), the entire diode array was used to scan the photocathode along the Y-axis and consequently map out the fluorescence distribution in the UV transmitting window.

Figure 7 shows a three-dimensional presentation of the counts accumulated in 10 diodes (Z-axis) plotted as a function of diode location (X-axis) and deflection position (Y-axis). These data were accumulated while the faceplate of the Digicon, which was oriented at an angle of -5.0 degrees, was bombarded with 32-Mev protons. The photocathode was at a potential of 20 kv with respect to the diode array. Clearly visible in the center of this area is a pronounced peak due to photoelectrons

released by UV luminescence photons created in the LiF window by the ionizing radiation. The high counts in diodes 11, 67, and 128 which seem to be independent of deflection position are due to protons that penetrate the LiF window and strike the left end of the diode array exposed to the beam at this angle. This was verified by turning the high voltage off (Figure 8), whereupon the photoelectron peak disappeared, leaving the other diodes unaffected. Small temporal variations in the beam flux caused the uneven appearance in this component. By moving the tube to -10.0 degrees, the diode array was completely removed from the path of the beam, isolating the luminescence peak (Figure 9) and allowing nearly background-free measurements of its magnitude.

Conversely, with the tube at 0.0 degrees and high voltage off, repeated scans with the deflection voltage off allowed plotting the diode counts as a function of diode location and time (Figure 10), where each substep represented an integration time per diode of 10 seconds. Here the peak was more poorly developed. Once again, the uneven structure along Y was due to beam variations, but the broadness of the structure along X was a result of the coulomb scattering of the collimated proton beam after passage through the 4-mm LiF faceplate. An increase of about 2.2 was estimated for the full width half maximum (FWHM). This is shown two-dimensionally in Figure 11.

Each deflection step covered 500 microns with 40 deflections resulting in a photocathode area of 20 by 22 mm being scanned. The area of the base of the peak in Figure 9 coincided roughly with the area of the beam spot (0.5 cm**2) estimated from pictures of the beam's cross section taken on polaroid film. This indicates that the fluorescence was confined to approximately that portion of the window through which the proton beam passed. There was essentially no demagnification in the mapping of the photoelectron image onto the diode array, hence each diode was receiving electrons from an area of the window comparable to the diode's area (8.5 x 10**-5 cm**2). Peak count rate occurred in diode 240 and was about 21 counts/sec, although 15 counts/sec was more typical of the Gaussian-like distribution. Here the proton flux was 82,000 p+/cm**2-sec.

Using this bombardment rate, and an accumulation time per deflection position of 10 seconds, we have estimated the apparent average magnitude of the luminescence in E3 (LiF/CsI) to be about two photoelectrons/proton-diode on the average, and at the central diode position, about three photoelectrons/proton-diode. Expressed differently, the average may be expressed as 1.6 * 10**-4 p.e./diode-proton-cm**2. (This result is normalized to the diode area specific to Digicon tubes E3 and E4). Averaging over the peak belt proton spectrum at the LiF window, a peak luminescence count rate is found to be 0.6 counts/diode-sec while in the belt. Averaging over the time spent in the belt yields 0.15 counts/diode-sec. The MgF2/CsTe tube produced similar results within the limits of experimental accuracy. These data are summarized along with other results in Table 1.

Diode Array Sensitivity

The assumption of an expected rate of one count per diode per incident proton was believed correct prior to these tests since (1) the energy deposited in each diode by a proton exceeds the threshold; (2) the electron-hole production by a single proton is almost instantaneous compared to the electronic resolving time; and (3) the average time between protons incident on a given diode is much greater than the resolving time. In order to check this hypothesis, we calculated the response of the

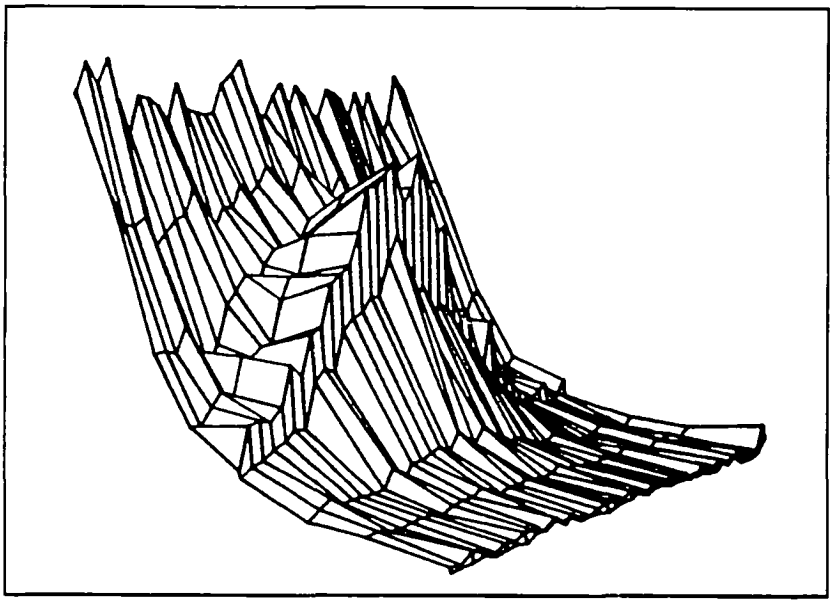

Figure 7. Counts (Z-axis) accumulated in each of 10 diodes of Digicon E3 plotted as a function of diode position (X-axis) and deflection position (Y-axis). The pronounced peak near the center is due to photoelectrons released by fluorescence induced by protons incident on the LiF window.

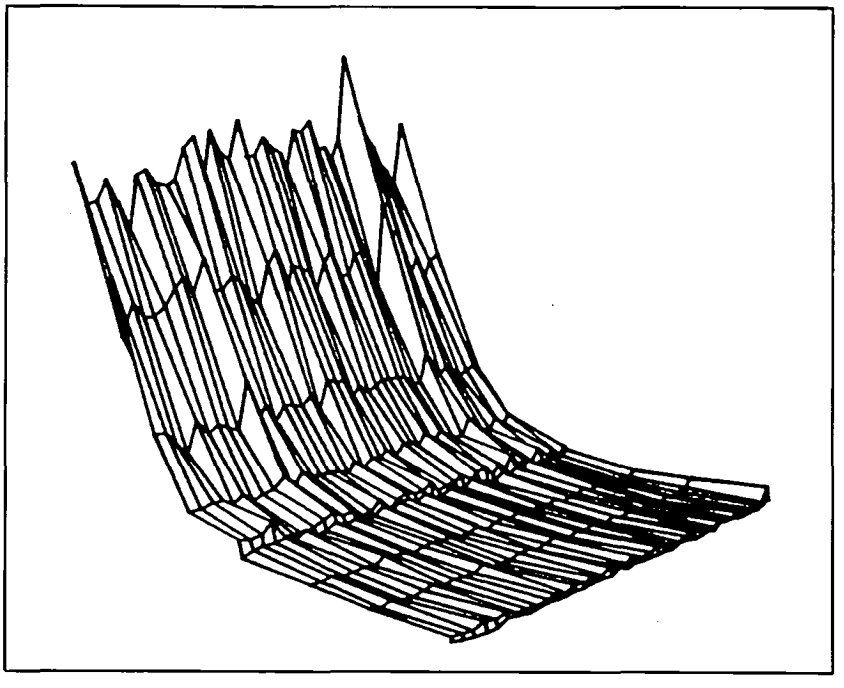

Figure 8. The same arrangement as for Figure 6 except that the accelerating voltage is off. Note that the peak near the center has vanished.

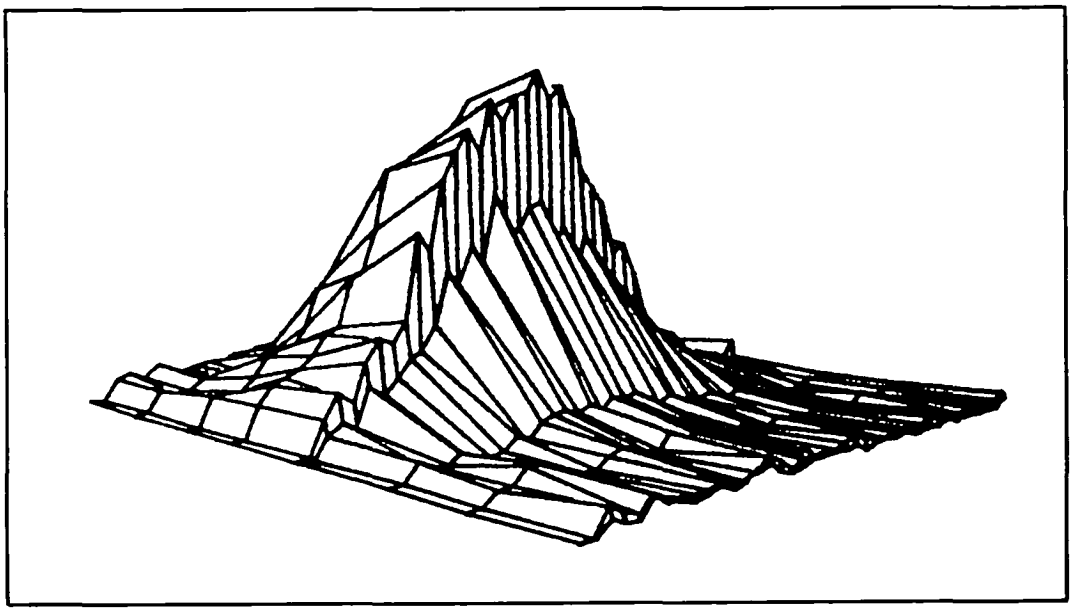

Figure 9. The same arrangement as in Figure 6 except that the diode array was well outside the direct proton beam.

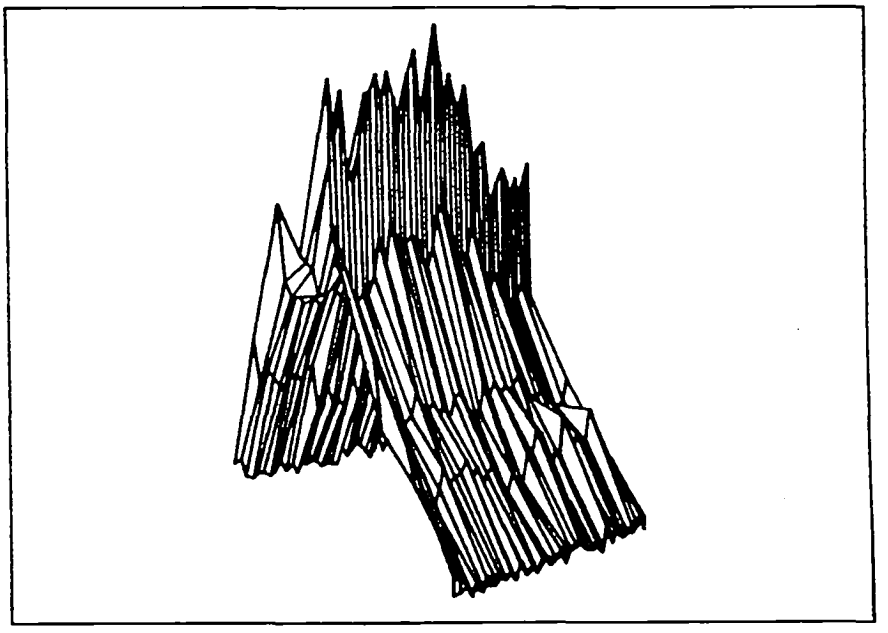

Figure 10. Diode counts (Z-axis) plotted as a function diode position (X-axis) and time (Y-axis) with the accelerating voltage and the deflection voltage off.

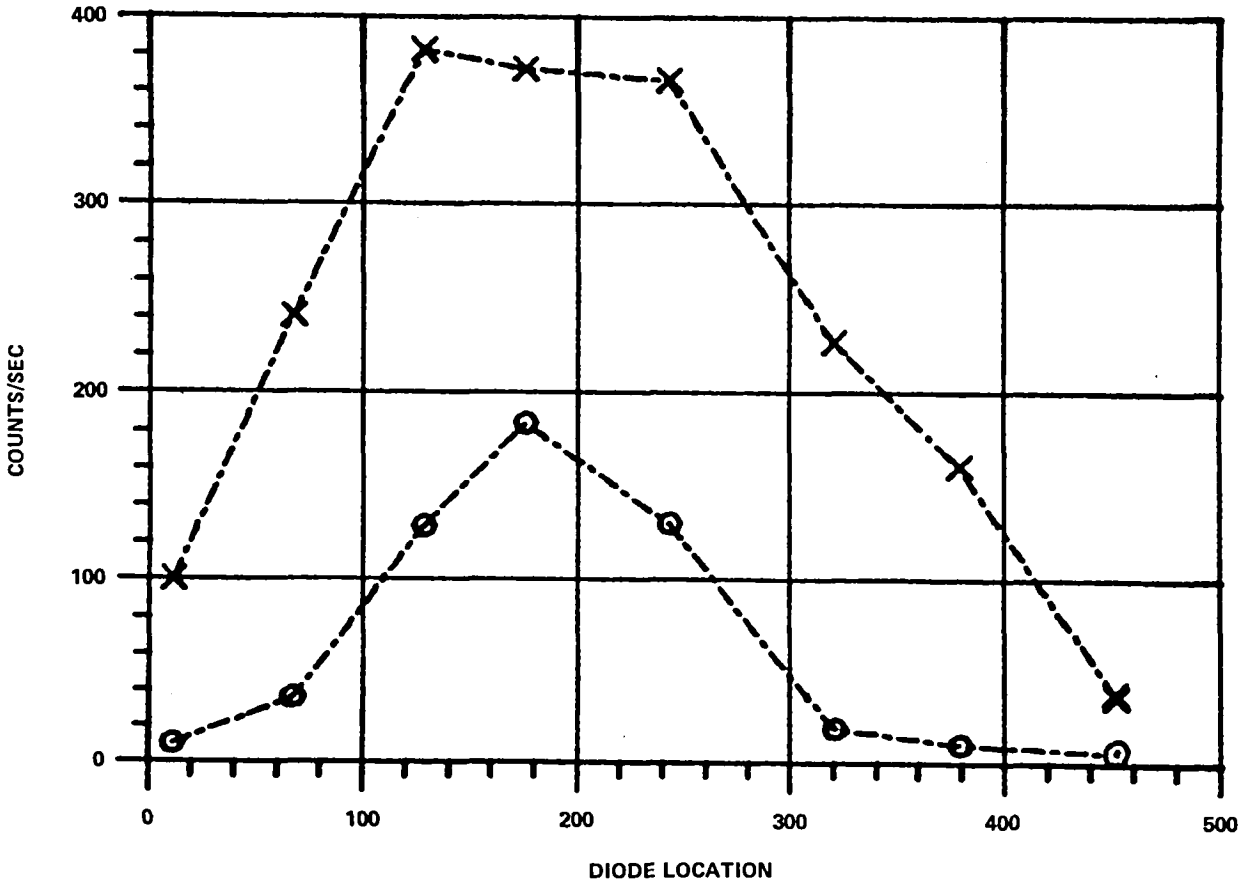

Figure 11. Diode counts versus location on array (Digicon E3). (X) represents counts induced by direct proton hits on diodes. HV off. (⊙) counts obtained by scanning faceplate with diode array while proton beam produces fluorescence in window. HV on. Counts not normalized to beam intensity.

diode array to direct proton bombardment by dividing the number of counts detected in each diode by the number of protons incident on the area of the diode during the same time. Each diode has an area of about 8,500 microns**2 and the flux at this small area could only be estimated through extrapolation of the counts measured at the SBD, and through use of the known area of the beam before passage through the faceplate and its subsequent spreading, described earlier. These factors were believed known within 10 percent, and were calculated as indicated in Table 1. Based on the assumption that each proton incident on the diode would produce exactly one count when bombarded with 20-Mev protons, a diode counting rate of about an order of magnitude larger than expected was obtained. This result is consistent with tests performed on a breadboard diode array (reported elsewhere[1]), and is believed to be due to diffusive collection of holes created by protons penetrating the low-resistivity bulk surrounding the diode depletion zone.

A similar effect has been observed using low-energy electron backside bombardment of thinned CCD arrays.[4,5,6] In both cases, it appears that the ionizing particle does not have to directly strike a diode to produce a count in that diode. Indeed, our results suggest that a 20-Mev proton can

Table 1
Window Responsivity and Diode Yield

Fluorescence Yield– – – 2-3 Counts/40-Mev Proton – Diode Area (±10%)
(1.6×10^{-4} Counts/Diode – 40-Mev Proton – Cm^2)
Diode Noise Yield – – – 10 Counts/Diode – 40-Mev Proton (±20%)
5 Counts/Diode – 85-Mev Proton (±20%)

Expected Peak Fluorescence Counts in SAA – – – – 0.5 Counts/Diode – sec
Expected Peak Diode Noise Counts in SAA – – – – 1.2 Counts/Diode – sec
Total 1.7 Counts/Diode – sec

Coincidence Fractions

Energy (Mev)	Diode Separation	Unshielded	30-Mil Aℓ Shield	90-Mil Aℓ Shield
40	1 (Adjacent)	0.28	0.31	0.37
	2	0.23	0.33	0.40
	3	0.13	0.15	–
	4	–	–	–
	5	–	–	–
	6	0.03	–	–
85	1	0.20		
	2	.077		
	6	.014		

enter the bulk up to 100 microns beyond a diode boundary and still induce a count there. Users of surface barrier detectors have observed pronounced diffusion collection from depths as great as 500 microns when these devices were irradiated with electrons.[7] The net result of this process is to increase the effective sensitive area of each diode to several times its actual dimensions. This, of course, is undesirable since it results in degraded signals to noise during passage through the SAA.

When the diode array was irradiated with 77-Mev protons, again at normal incidence, the enhanced count rate was present, although to a lesser degree. Only 4.5 times as many counts were induced in each diode as would be expected based on diode area alone. In fact, the ratio of diode-effective sensitive area at 20 Mev to that at 77 Mev was in the same ratio as the specific ionization loss for the proton at the respective energies. This reinforces the ionized electron-hole pair/diffusive collection hypothesis.

Shown in Table 1 is a conservative estimate of the number of proton-induced diode counts expected on the basis of the anticipated proton flux density of 4,000 p+/cm**2/sec at the diode array, and

using the above result of between 5 and 10 counts/proton-diode. Earlier projections had placed the expected background at 0.5 counts/diode-sec, using an anticipated proton flux of 10**4 p+/cm**2/sec.[8]

The need for further analysis of the diode array's dynamical charge collection characteristics led to the second series of tests conducted on Digicon E4. Here the emphasis was on evaluating the relation between the p-n junction/substrate combination and charge deposited within this structure by normally incident protons. For this purpose several test categories were established:

- Pulse-height analysis of proton-induced diode counts
- Multidiode coincidence measurements
- Shielding test

Pulse-Height Analysis

Knowledge of the pulse-height distribution of counts induced by protons striking the diode array was believed to be valuable in several respects, since:

- Insufficient data existed on the charge collection characteristics of the p-n junction/substrate combination, preventing realistic evaluation of the response of the diode array to proton bombardment.
- Designers of background rejection circuitry could benefit directly from a knowledge of the amplitude distribution of the counts.

Shown in Figure 12 is a pulse-height distribution of photoelectrons collected by a typical diode and produced by exposing the MgF2/CsTe faceplate on the E4 tube to a UV penlight located several centimeters away. The peak of the distribution falls around channel 90, with the FWHM around 30 channels. This indicates a resolution of about 35 percent, which is nominal, considering that the depletion depth of the diode (2-3 microns) is barely enough to absorb a 20-kev electron. The low-energy tail is expected on the basis of surface backscattering, and photoelectrons striking diode boundaries, both of which cause electrons to deposit less than their full energies inside the diode.

In the latter case, since only 10 microns separate one diode boundary from another, it is likely that photoelectrons landing near diode boundaries generate a charge that is shared among several diodes. In fact, only those photoelectrons which strike a diode dead center could be expected to have a significant probability of depositing their total energy inside the diode. Therefore, due to the lack of an independent charge calibration of the preamp, which was not feasible during this test setup, a value to the peak cannot be assigned. All pulse-height distributions presented have the horizontal axis calibrated in relative units with respect to the photoelectron peak, which is assigned the value of 1.

Pulse-height distributions of counts produced by direct proton bombardment of the diode array are shown for the same diode in Figure 13. Proton primary energy was 40 Mev (20 Mev at the diode

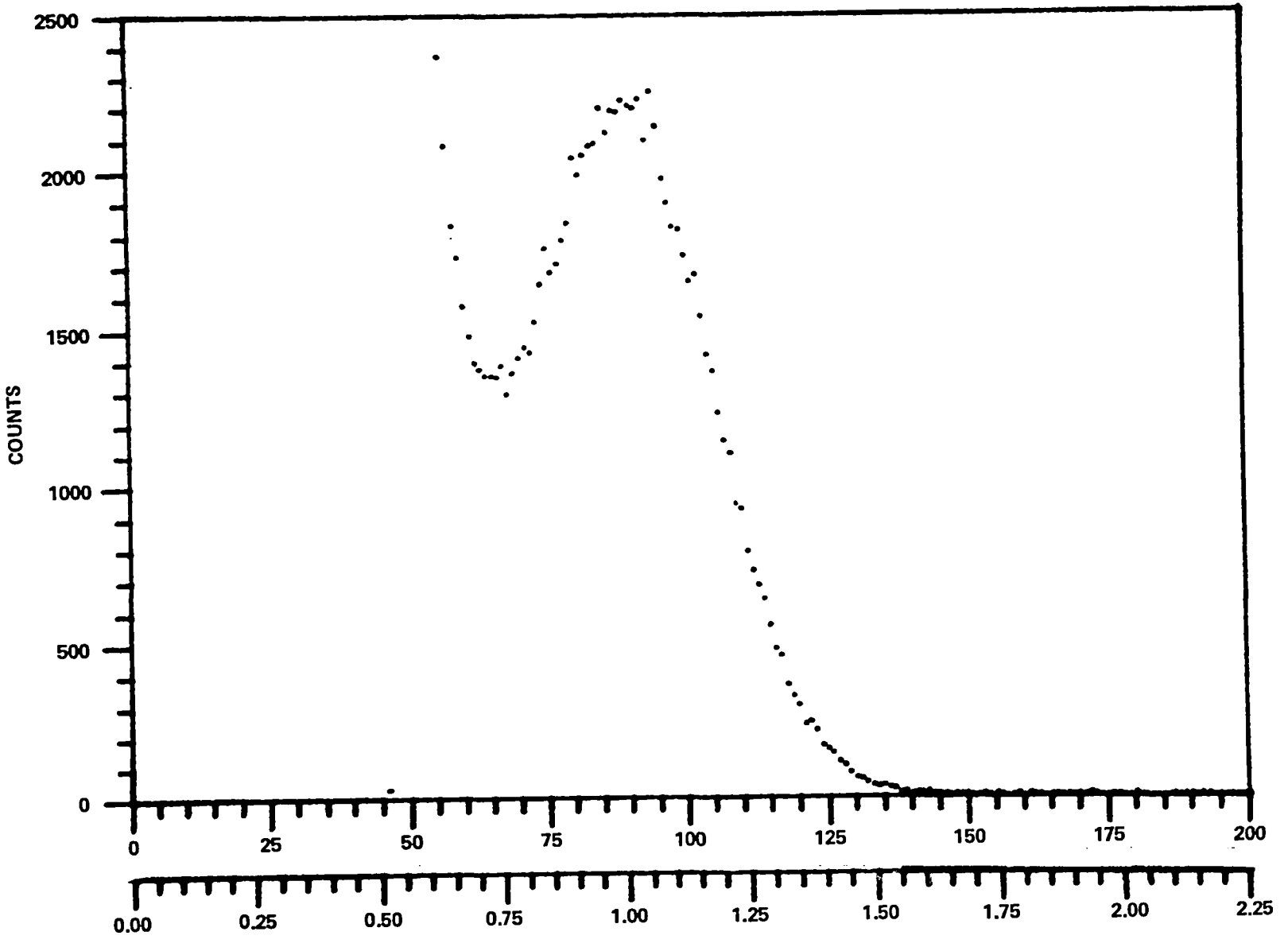

Figure 12. Pulse-height distribution of photoelectrons collected by one diode of Digicon E4 when a UV penlight was placed several centimeters in front of the Digicon.

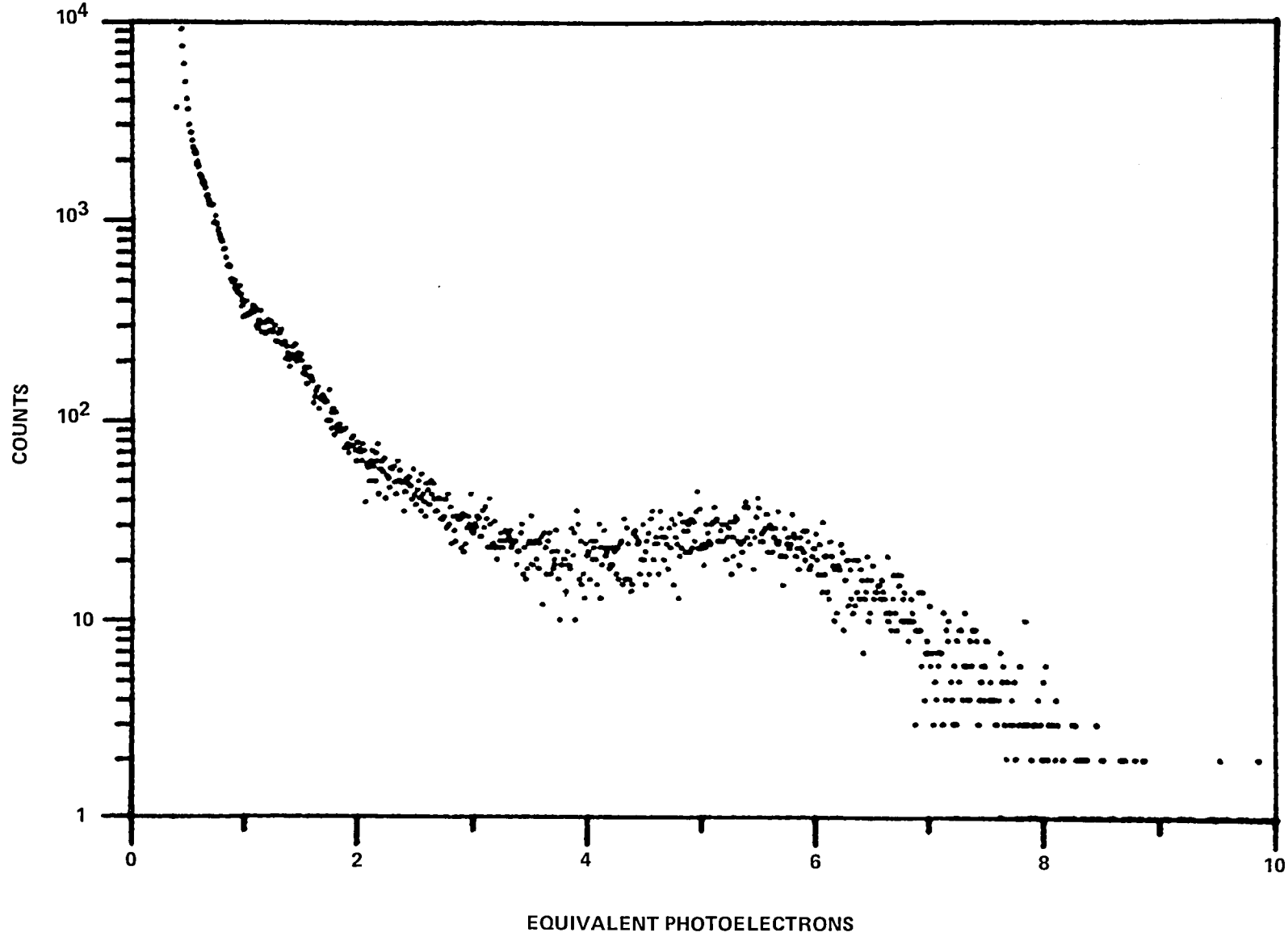

Figure 13. Pulse-height distribution of counts induced in the same diode as Figure 12, using direct proton bombardment of diode array. Digicon E4 was aligned with the 40-Mev proton.

array). This distribution is typical of the response seen in all the diodes, and has been observed previously during proton bombardment[1] and when using low-energy electrons.[4] Predominating the distribution are the counts between the noise level and 3.6 equivalent photoelectrons, terminating in a broad peak at around 5.3. A 20-Mev proton passing through the 2-3 micron depletion layer would deposit no more than 4,000 electron-hole pairs, which is comparable to the expected photoelectron value. Therefore, since the peak at 5.3 has to be associated with the energy loss of the primary proton, it appears likely that charge pairs created outside of the depletion layer are largely responsible. No other likely explanation for this peak is apparent, and this interpretation has been adopted. Therefore, the portion of the distribution between the noise level and 3.6 is attributed to be the result of charge diffusing from ionization trails left by protons penetrating the bulk at points exterior to the diode boundaries. This would explain the anomalously high count rate described earlier as being due to an increase in the effective area of each diode. Protons penetrating the diode and continuing on beneath would create charge which would rapidly diffuse upwards and add to the 4,000 e-h pairs created in the depletion layer, thus producing the peak seen in the region of 5.3 equivalent photoelectrons.

Irradiation of the tube at 85-Mev primary beam energy (77 Mev at the diode array) resulted in a pulse-height spectrum typical of that shown in Figure 14. Although the position of the peak has decreased by a factor of nearly three, the counts are still clearly above the photoelectron peak and well above the noise level. The factor-of-three reduction in peak location can be attributed to the lower specific ionization loss of the 77-Mev proton (1.65 kev/micron) as compared to a 20-Mev proton (4.72 kev/micron), with nearly three times less charge deposited over the same path length.

Multidiode Coincidence Measurements

As these pulse-height spectra indicate, protons irradiating the diode array create background counts having amplitudes which overlap the spectral region containing the single photoelectron peak. Hence, use of the Digicon in such an environment would lead to reduced signal-to-noise, unless selective measures were undertaken to prevent the accumulation of these proton-induced counts during data taking. One such method involves the use of lower level and upper level discriminators which can reject counts having pulse amplitudes greater than or less than a preset level. This would restrict the range of acceptable pulses to include only those falling within the peak shown in Figure 12. However, a substantial portion of background counts would fall within this window, and some other method must be employed.

The close proximity of one diode to another, as well as the observation that the effective area of adjacent diodes overlapped, suggested that charge could leak to several diodes within a very short time interval, and thus create counts in adjacent diode pairs nearly coincidentally. This has indeed been observed in a 250-micron-thick CCD array exposed to highly ionizing cosmic rays, whereby dozens of pixels were simultaneously activated.[6] This has suggested that the use of anticoincidence-pulse-rejection techniques, already being considered for use in the Digicon electronics package, may serve to enhance the s/n ratio. To study this effect, signal lines were connected from various combinations of diode pairs into a coincidence circuit with a one microsecond window. This unit produced one count for every count which occurred in both diodes within one microsecond of each other. It was expected that the greater the distance separating the diode pairs,

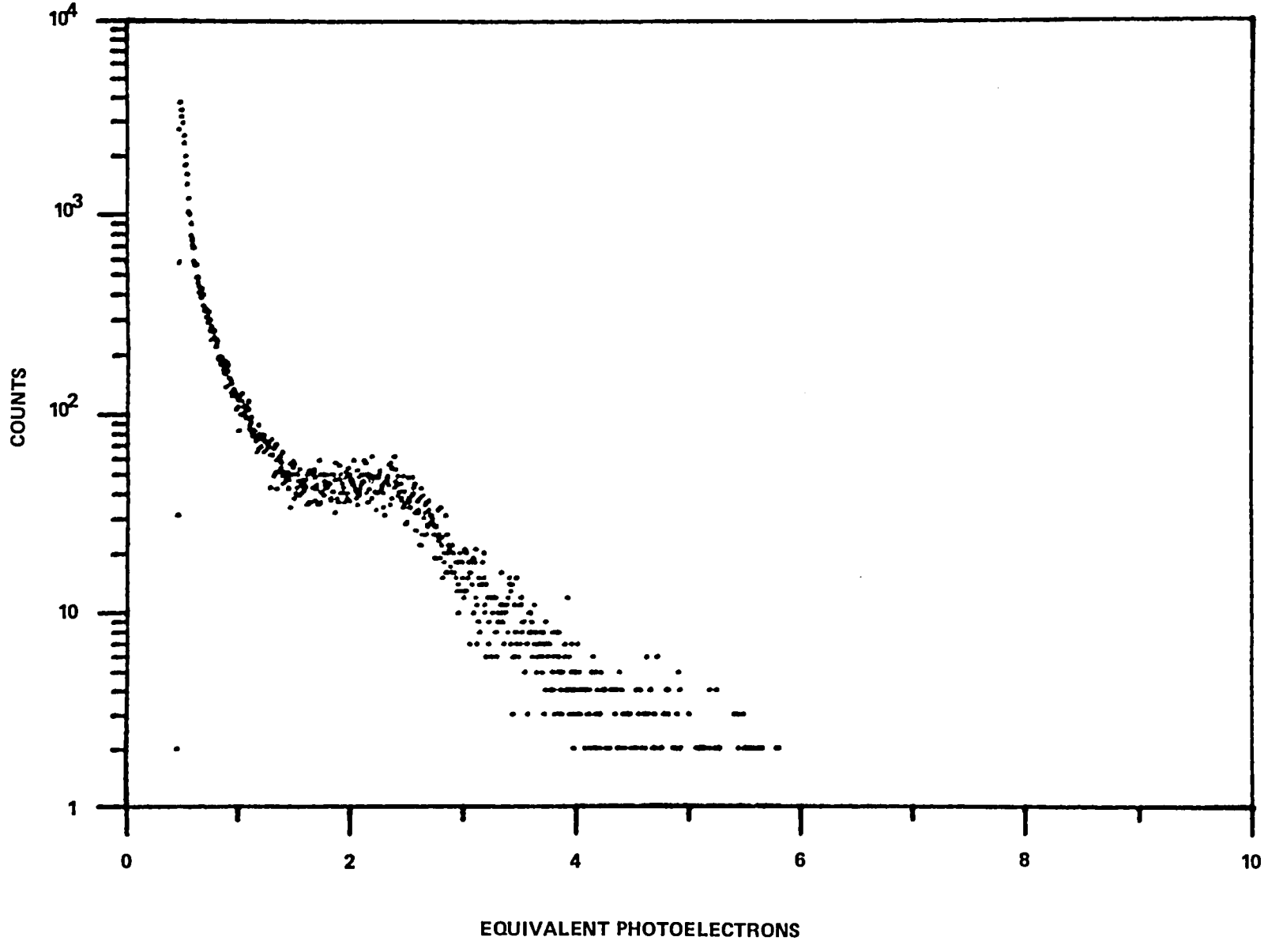

Figure 14. The same arrangement as Figure 12, using an 85-Mev incident proton beam.

the smaller would be the coincidence rate as the diffusing charge would have dispersed over a large area, resulting in less charge reaching both diodes.

The coincidence response of one diode with respect to another, has been defined by dividing the total number of coincidence counts occurring between the two diodes during an arbitrary time interval by the average number of total counts obtained from both diodes during the same interval. Shown in Figure 15 is a plot of this fraction as a function of diode separation, for both 40-Mev and 85-Mev primary beam energy. The largest coincidence fraction measured was for adjacent diodes, about 28 percent, which means that 28 percent of the proton-induced counts in one diode occur simultaneously in the other because they are, presumably, due to the same proton. As expected, the coincidence response falls off with increasing diode separation; the largest value always occurs for adjacent diodes, although there is a measurable effect up to six diode spacings apart. Also indicated in Figure 15 is the strong energy dependence of the coincidence. This is expected, due to the specific ionization loss of the proton being less at higher energies, thus producing less charge per unit length to be shared among the diodes. At energies below 20 Mev, larger coincidence fractions are to be expected.

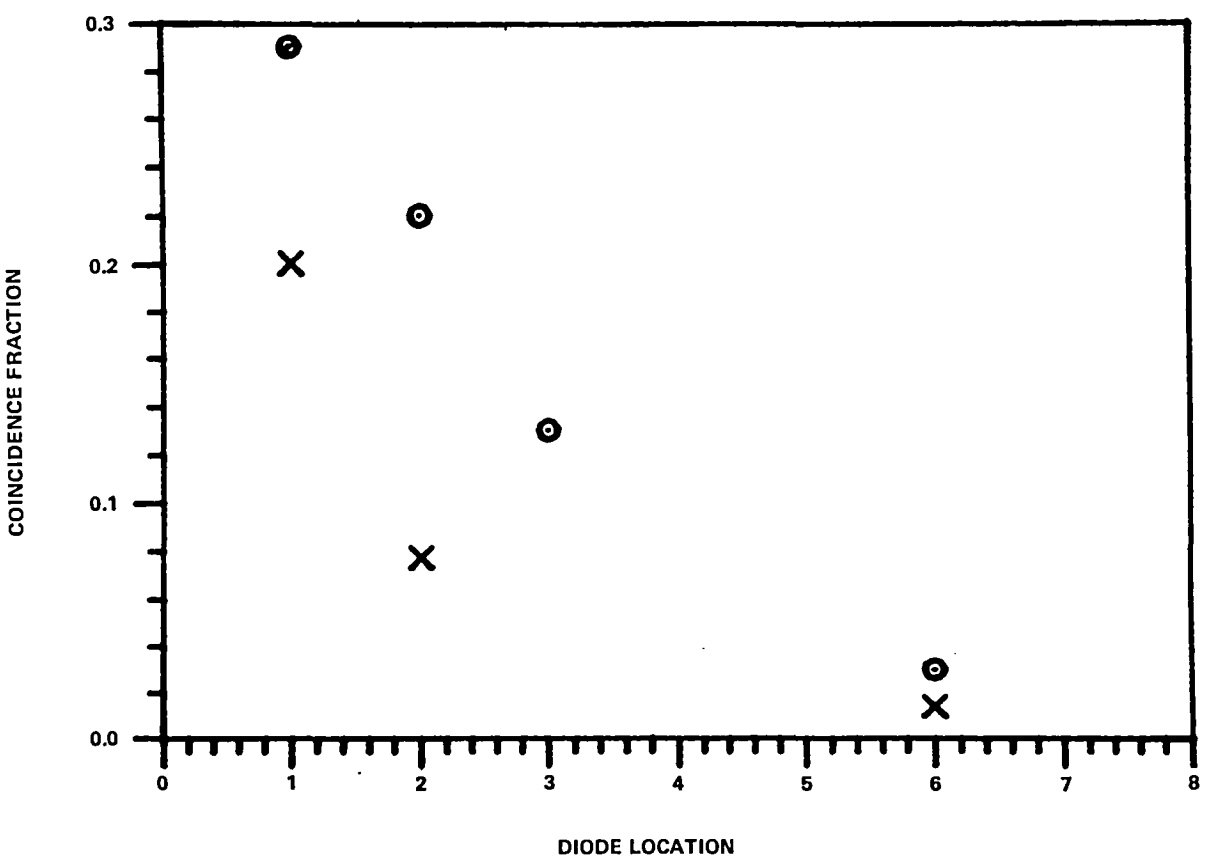

Figure 15. The ratio of coincidence counts to total counts observed for a pair of diodes plotted versus separation of the diodes for bombarding proton energies of 40 Mev (circles) and 85 Mev.

Since the coincidence response for a given pair of diodes is presumably proportional to the extent to which each diode's effective sensitive area overlaps the other's, it should be possible to establish a dependence of this response on the geometrical arrangement of the diodes on the array. To experimentally verify this dependence we performed a two-parameter analysis using the IBM 360/44 data acquisition system available to users of the cyclotron. In this experiment, signals from a pair of diodes were each sent to separate analog-to-digital converters. If the conversion in one ADC occurred within 40 microseconds of that occurring in the other, both events were registered as a coincidence and sent to a dual parameter and display controller where the events were plotted and then stored on magnetic tape. A Z-intensified contour display of several diode pairs is shown in Figure 16.

In each display, the counts in one diode are plotted versus the counts in the other, and only those counts which occurred in coincidence are plotted. The intensity of the data points is proportional to the number of counts each point represents. As Figure 16a shows, for adjacent diodes high-amplitude counts in one diode were in coincidence with low-amplitude counts in the other. This pattern was representative of diode pairs separated by zero or two diodes. Pairs separated by one diode displayed different characteristics, as shown in Figure 16b. Here low-amplitude counts in one diode coincided with low-amplitude counts in the other diode. This pattern is believed to be related to the alternating fashion in which the diodes are ordered (see Figure 3).

Pulse-height distributions of counts occurring in coincidence were obtained by using the output of the coincidence unit to gate open a multichannel analyzer. This produced a spectrum from one diode of only those counts received in both diodes simultaneously. Such a spectrum for a typical pair of adjacent diodes is shown in Figure 17, and reveals that most of the coincidence pulses overlap the single photoelectron peak position.

In conclusion, although a substantial fraction of proton-induced diode array counts can be effectively rejected through anticoincidence techniques, actual performance of such methods depends on several factors:

- Geometrical arrangement of diodes in the array
- Energy spectrum of protons incident on the array
- Coincidence rejection thresholds
- Effective use of lower and upper level discriminators

Shielding

The effects of various thicknesses of aluminum shielding were examined by placing 30-mil sheets of aluminum plate between the solid state detector and the Digicon faceplate. Degradation of both beam energy and collimation resulted in an expected smearing of the pulse-height distribution of diode array counts, as well as marked increase in the coincidence rate between diode pairs. This latter effect, as mentioned previously, results from a greater density of electron-hole pairs per unit length produced by the degraded protons having larger dE/dX. For adjacent diode pairs, placing

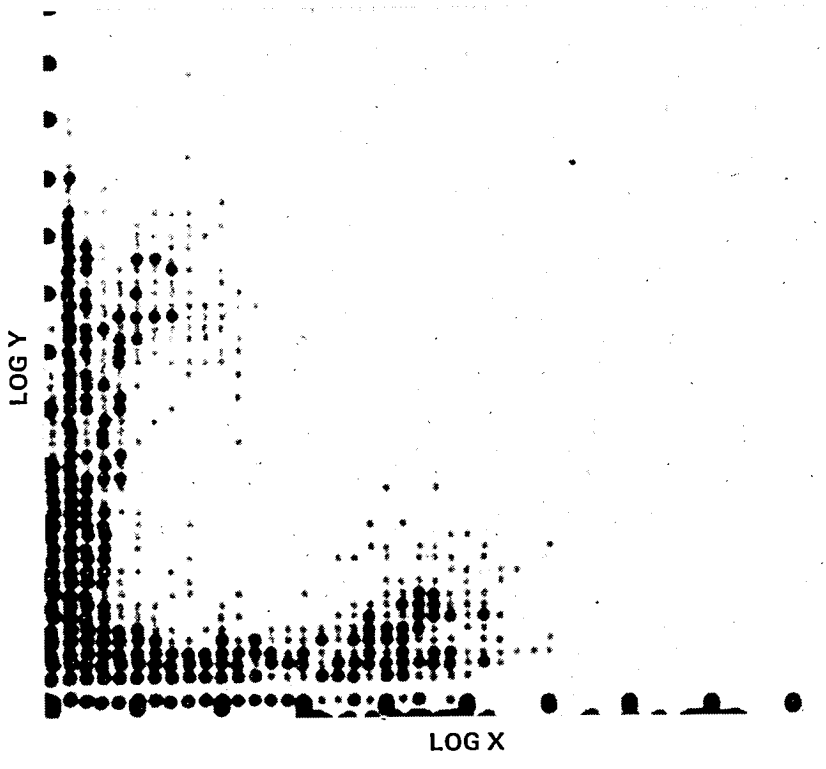

(a)

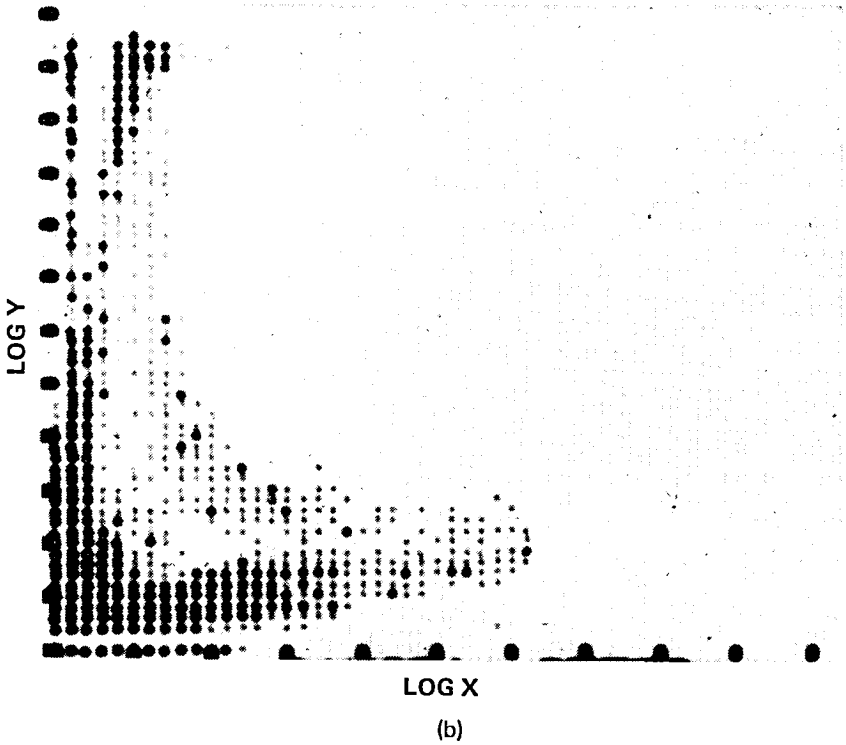

(b)

Figure 16. A Z-intensified contour of pulse height of coincident pulses in one diode versus pulse height of coincident pulses in a second diode. 16a is for a pair of diodes separated by an even number of diodes while 16b is for a pair separated by an odd number of diodes.

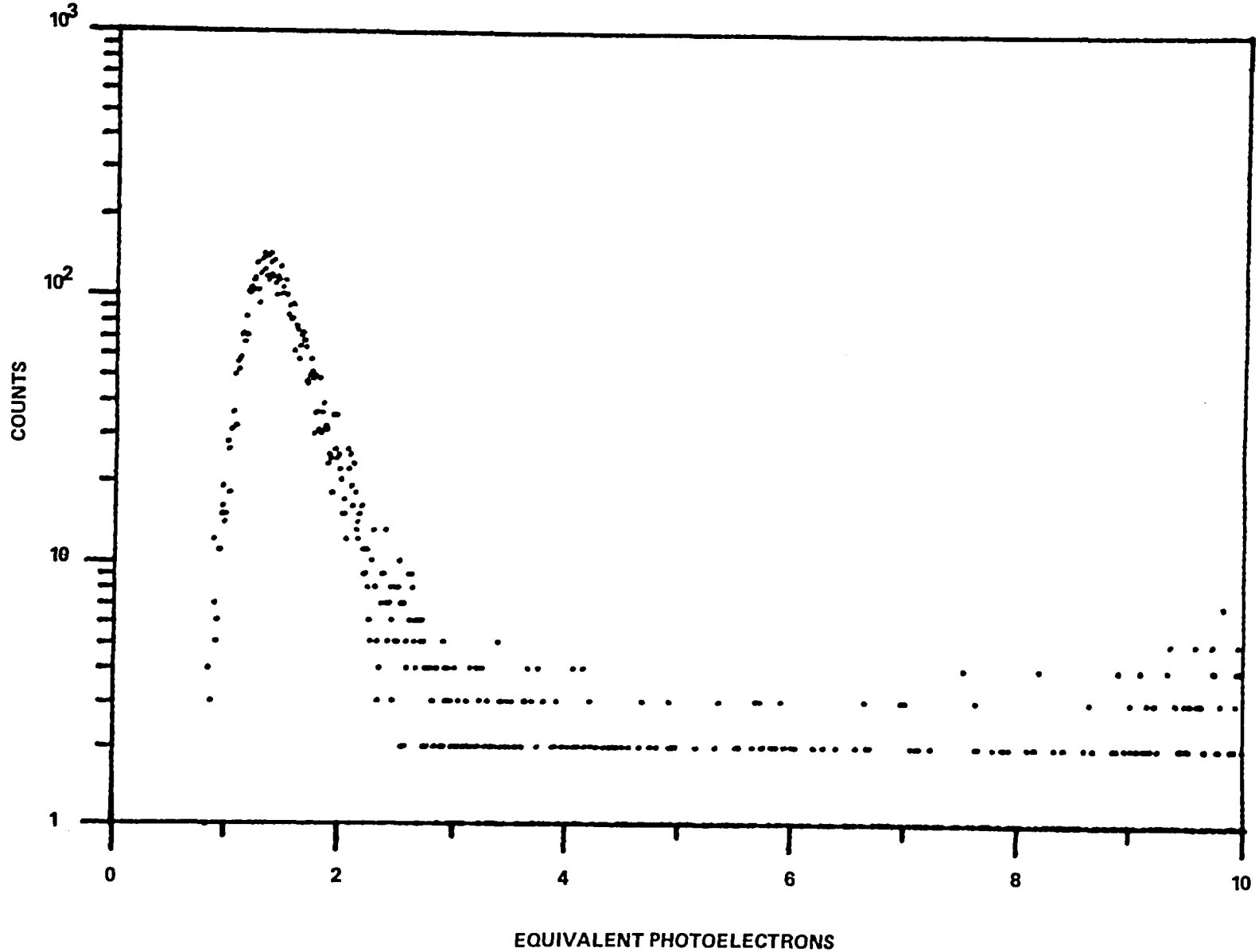

Figure 17. Pulse-height distribution of pulses in one diode which are in coincidence with pulses in a neighboring diode.

three thicknesses of 30-mil aluminum in the 40-Mev p+ beam increased the coincidence fraction from 28 percent to nearly 40 percent.

SUMMARY

These measurements have shown that the Space Telescope/HRS Digicon, when exposed to medium-energy protons, exhibits background noise from fluorescence induced in the Digicon faceplate, and from direct proton bombardment of the diode array. The magnitude of the latter effect exceeds earlier estimations by a factor of between 5 and 10. Crosstalk has also been observed between diodes separated by as much as 250 microns, although the extent of this effect is tied closely to such parameters as the pattern of diode placement on the array. From these models, as well as the work of others, it is believed that other parameters influencing these proton/diode array effects include: bulk thickness, diode area, trapping center lifetimes, preamplifier time constants, and proton energy. Further studies into these mechanisms should yield insight as to a means of reducing the magnitude of these noise sources, as well as provide information useful to designers of future photodiode sensors.

REFERENCES

1. Becher, J., R. L. Kernell, C. S. Reft and L. C. Smith, "Radiation Effect Studies for the High Resolution Spectrograph," Technical Report PTR-80-2, Old Dominion University, Norfolk, Virginia, 1980.

2. Brandt, J. C., A. Boggess, S. R. Heap, S. P. Maran and A. M. Smith, "High Resolution Spectrograph for the Space Telescope," *Proceedings SPIE Instrumentation in Astronomy III*, Tucson, Arizona, p. 254, Vol. 172, January 1979.

3. Kelsall, T., "Detectors for the Space Telescope," *Proceedings SPIE Applications of Electronic Imaging Systems,* Vol. 143, p. 27, 1978.

4. Hier, R. G., E. A. Beaver and G. W. Schmidt, "Photon Detection Experiments with Thinned CCDs," *Advances in Electronics and Electron Physics*, Vol. 52, pp. 463-480, 1979.

5. Lowrance, J. L., P. Zucchino, G. Renda and D. C. Long, "ICCD Development at Princeton," *Advances in Electronics and Electron Physics*, Vol. 52, pp. 441-452, 1979.

6. Marcus, S., R. Nelson and R. Lynds, "Preliminary Evaluation of a Fairchild CCD-211 and a New Camera System," *Proceedings SPIE Instrumentation in Astronomy III*, Vol. 172, pp. 207-218, January 1979.

7. Walter, F. J. and R. R. Boshart, "Low Background Counting of Betas and Alphas with Silicon Detectors," *Nuclear Instruments and Methods*,Vol. 42; No. 1, pp. 1-14, 1966.

8. Brandt, J. C., "A High Resolution Spectrograph for the Space Telescope," HRS-680-77-01, NASA, 1977.

1. Report No. NASA TP-1852	2. Government Accession No.	3. Recipient's Catalog No.
4. Title and Subtitle Proton-Induced Noise in Digicons		5. Report Date August 1981 6. Performing Organization Code
7. Author(s) L. Cole Smith, Jacob Becher, Walter B. Fowler, and Keith Flemming		8. Performing Organization Report No. 81F0051
9. Performing Organization Name and Address Goddard Space Flight Center Greenbelt, Maryland 20771		10. Work Unit No. 11. Contract or Grant No. 13. Type of Report and Period Covered Technical Paper
12. Sponsoring Agency Name and Address National Aeronautics and Space Administration Washington, D.C. 20546		14. Sponsoring Agency Code

15. Supplementary Notes

L. Cole Smith and Jacob Becher: Old Dominion University, Norfolk, Virginia.
Walter B. Fowler and Keith Flemming: Goddard Space Flight Center.

16. Abstract

The Space Telescope (ST), which carries four Digicons, will pass several times per day through a low-altitude portion of the radiation belt called the South Atlantic Anomaly (SAA). This is expected to create interference in what is otherwise anticipated to be a noise-free device. Two essential components of the Digicon, the semiconductor diode array and the UV transmitting window, generate noise when subjected to medium-energy proton radiation, a primary component of the belt. These trapped protons, having energies ranging from 2 to 400 Mev and fluences at the Digicon up to 4,000 P+/sec-cm^2, pass through both the window and the diode array, depositing energy in each.

In order to evaluate the effect of these protons, engineering test models of Digicon tubes to be flown on the High Resolution Spectrograph (HRS) were irradiated with low-flux (10^4 - 10^5 P+/sec-cm^2) monoenergetic proton beams at the University of Maryland cyclotron. Electron-hole pairs produced by the protons passing through the diodes or the surrounding bulk caused a background count rate. This is the result of holes diffusing over a distance of many diode spacings, causing counts to be triggered simultaneously in the output circuits of several adjacent diodes. Pulse-height spectra of these proton-induced counts indicate that most of the bulk-related counts overlap the single photoelectron peak. A geometrical model will be presented of the charge collection characteristics of the diode array that accounts for most of the observed effects.

17. Key Words (Selected by Author(s))	18. Distribution Statement
Spacecraft Detectors Proton Noise	Star Category 19 Unclassified - Unlimited

19. Security Classif. (of this report)	20. Security Classif. (of this page)	21. No. of Pages	22. Price*
Unclassified	Unclassified	33	A03

*For sale by the National Technical Information Service, Springfield, Virginia 22161.

NASA-Langley, 1981

National Aeronautics and Space Administration

Washington, D.C.
20546

Official Business
Penalty for Private Use, $300

THIRD-CLASS BULK RATE

Postage and Fees Paid
National Aeronautics and
Space Administration
NASA-451

NASA

POSTMASTER: If Undeliverable (Section 158 Postal Manual) Do Not Return